① Wilson & Gray Report
② Steward & Mones

UCRL-JC-124602
PREPRINT

Comparison and Modeling of Aqueous Dissolution Rates of Various Uranium Oxides

S. A. Steward
E. T. Mones

This paper was prepared for submittal to the
Materials Research Society Fall Meeting
December 2-6, 1996
Boston, MA

November 1996

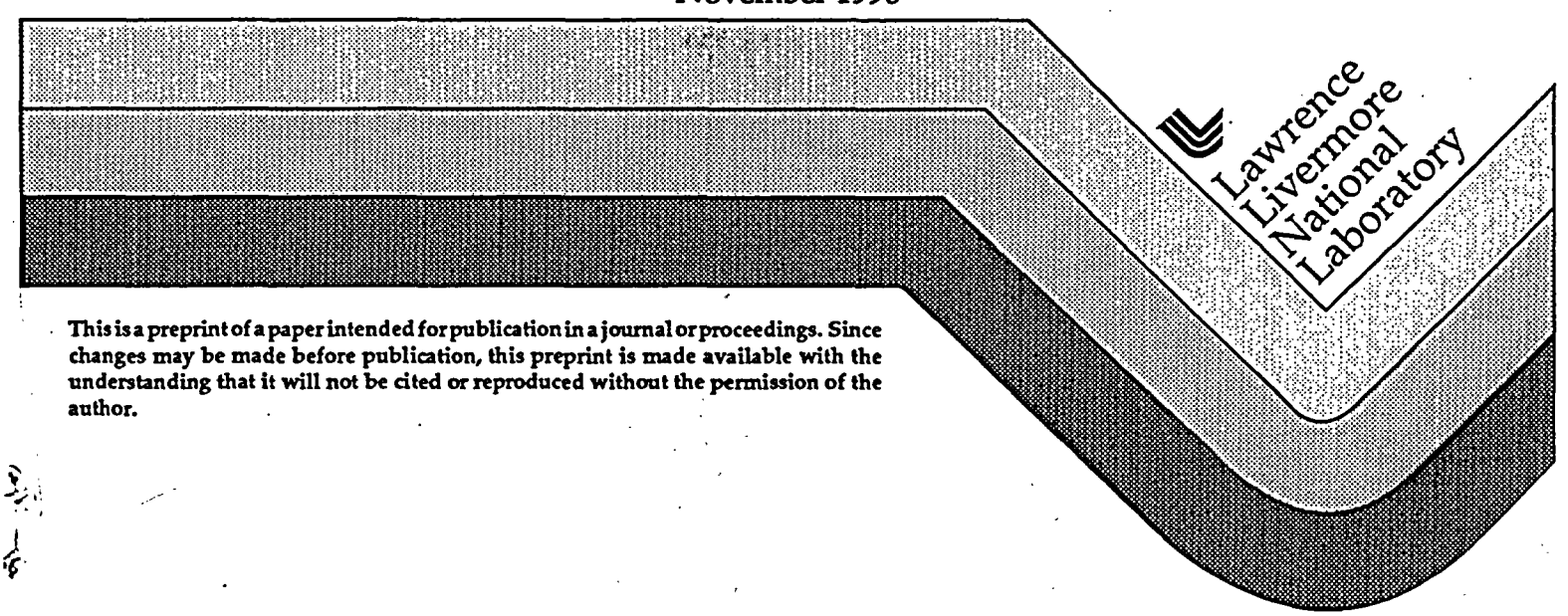

This is a preprint of a paper intended for publication in a journal or proceedings. Since changes may be made before publication, this preprint is made available with the understanding that it will not be cited or reproduced without the permission of the author.

Lg09-20

DISCLAIMER

This document was prepared as an account of work sponsored by an agency of the United States Government. Neither the United States Government nor the University of California nor any of their employees, makes any warranty, express or implied, or assumes any legal liability or responsibility for the accuracy, completeness, or usefulness of any information, apparatus, product, or process disclosed, or represents that its use would not infringe privately owned rights. Reference herein to any specific commercial products, process, or service by trade name, trademark, manufacturer, or otherwise, does not necessarily constitute or imply its endorsement, recommendation, or favoring by the United States Government or the University of California. The views and opinions of authors expressed herein do not necessarily state or reflect those of the United States Government or the University of California, and shall not be used for advertising or product endorsement purposes.

$e^{-10/2} = 6.7 \times 10^{-3}$ $\quad e^{-10/3} = 3.6 \times 10^{-2}$

$e^{-20/2} = 4.5 \times 10^{-5}$ $\quad e^{-20/3} = 1.3 \times 10^{-3}$ $\quad \times 29$

$\log R = -2130/T$

$\frac{1}{2.3} \Rightarrow \log \ln Y = -2130/T$

$\times 3.4 \quad \ln Y = \frac{2.3 \times 2130}{T} \frac{273}{25}$

$\ln r = 2.303 \log s$

(40)

$2130/298 = 6.81 \log(298) \cdot \log(0.2) = X/298$

$X = 2130 - 298 \times 6.81 \times \log(298) \cdot \log(0.2)$

$= 2130 + 3514 \quad 2.474 \quad (-0.70)$

$=$

COMPARISON AND MODELING OF AQUEOUS DISSOLUTION RATES OF VARIOUS URANIUM OXIDES

S. A. STEWARD and E. T. MONES
Lawrence Livermore National Laboratory, P.O. Box 808, Livermore, CA 94550

ABSTRACT

The purpose of this work has been to measure and model the intrinsic dissolution rates of uranium oxides under a variety of well-controlled conditions that are relevant to a geologic repository. When exposed to air at elevated temperature, spent fuel may form the stable phase U_3O_8. Dehydrated schoepite, $UO_3 \cdot H_2O$, has been shown to exist in drip tests on spent fuel.

Equivalent sets of U_3O_8 and $UO_3 \cdot H_2O$ dissolution experiments allowed a systematic examination of the effects of temperature (25-75°C), pH (8-10) and carbonate (2-200x10^{-4} molar) concentrations at atmospheric oxygen conditions.

Results indicate that $UO_3 \cdot H_2O$ has a much higher dissolution rate (at least ten-fold) than U_3O_8 under the same conditions. The intrinsic dissolution rate of unirradiated U_3O_8 is about twice that of UO_2. Dissolution of both U_3O_8 and $UO_3 \cdot H_2O$ shows a very high sensitivity to carbonate concentration. Present results show a 25 to 50-fold increase in room-temperature $UO_3 \cdot H_2O$ dissolution rates between the highest and lowest carbonate concentrations.

As with the UO_2 dissolution data the classical observed chemical kinetic rate law was used to model the U_3O_8 dissolution rate data. The pH did not have much effect on the models, in agreement with the earlier analysis of the UO_2 and spent fuel dissolution data,. However, carbonate concentration, not temperature, had the strongest effect on the U_3O_8 dissolution rate. The U_3O_8 dissolution activation energy was about 6000 cal/mol, compared with 7300 and 8000 cal/mol for spent fuel and UO_2 respectively.

INTRODUCTION

Understanding the long-term dissolution of spent fuel in groundwater is necessary for its safe disposal in a geological repository. Radionuclides could be released from such a repository by dissolution and transport processes in flowing groundwater. The dissolution of the UO_2 spent fuel matrix is regarded as the rate-limiting step for release of radioactive fission products. Therefore, the intrinsic UO_2 dissolution rate sets an upper limit on the aqueous radionuclide release rate. If the UO_2 in the spent fuel matrix contacts air and is oxidized further, then these dissolution responses also must be measured.

It is commonly assumed that oxidized fuel would dissolve faster than its unoxidized predecessor. The purpose of this and previous work has been to measure the intrinsic dissolution rates of uranium oxides, as well as unoxidized and oxidized spent fuel, under a variety of well-controlled conditions that are relevant to a geological repository and allow for subsequent modeling. When exposed to air at elevated temperature, spent fuel may form the stable phase U_3O_8. A form of the trioxide, dehydrated schoepite, $UO_3 \cdot H_2O$, has been shown to exist in drip tests on spent fuel [1]. The results of essentially identical dissolution experiments performed on depleted U_3O_8 and $UO_3 \cdot H_2O$ will be compared. These are in turn compared with earlier work on spent fuel and UO_2 under similar conditions [2].

Water from wells near Yucca Mountain contain typical aqueous constituents, such as carbonates, sulfates, chlorides, silicates, and calcium. Of the anions commonly found in groundwater, bicarbonate is considered to be the most aggressive towards uranium oxides, forming complexes with the uranyl (UO_2^{+2}) cation. This makes the carbonates good surrogates for all anions in aggressive groundwater. Statistical experimental design was used to plan the set

of U_3O_8 and $UO_3 \cdot H_2O$ dissolution experiments. This approach allows a systematic examination of the effects of temperature, pH and carbonate concentrations on the dissolution rates of these two oxides. It also minimizes the number of experiments required, and provides a robust data set suitable for modeling and comparison with the previously reported UO_2 dissolution data. Because of the already elevated oxidation state, these experiments were run only at 8 ppm dissolved oxygen in the leaching solutions, equivalent to 0.2 atmosphere oxygen in air. The dissolution rates from the design allow a fit to a second-order model in all variables, including interactions between the variables. Additional experiments on UO_2 complete a matrix of dissolution rates measured on all three oxides at the same conditions.

EXPERIMENTAL

As with previous studies [2,3,4], the intrinsic dissolution rates of the uranium oxides were determined by using a single pass flow-through method. Flow rates and specimen size can be controlled with this approach so that the oxides dissolve under conditions that are far from solution saturation (no precipitation of dissolved products). Thus, the dependence of UO_x dissolution kinetics on pH, temperature, oxygen and carbonate/bicarbonate concentrations can be evaluated.

Experiments at three different values of each variable were required, in order to test for nonlinear effects of the three variables on the uranium dissolution rates. The chosen variable ranges were pH's of 8 to 10, temperatures of 25° to 75°C, total carbonate concentrations of 0.2 to 20 millimol/L and 8 ppm dissolved oxygen. The carbonate concentrations bracketed the typical groundwater concentration of 1 millimol/L. The pH range covered a value typical of groundwaters (pH=8) to very alkaline conditions. The dissolved oxygen concentration is the value at atmospheric pressure.

A model that can discriminate nonlinear effects and interactions of the three variables for both oxides has at least 14 terms. A sixteen experiment design is, therefore, the minimum number of experiments required for a numerical regression fit, with extra degrees of freedom to account for experimental variability. For each oxide, a classical three-level, full-factorial experimental design consists of the 27 (3^3) possible combinations of variable settings from the three variables at low, medium and high values. Performing such a large number of 54 experiments was unrealistic. The first 16 experiments listed in Table 1 are a D-optimal design chosen using the RS/Discover computer program from BBN Software [5]. This group represents one of many equivalent designs that could be picked from the candidate set of 54 experiments. For example, if the experiments for the two oxidation states were reversed, an equally good design would result.

The first eight experiments in Table 1, four for each oxide, are a screening design that tests whether each variable has any significant effect on dissolution rate. The D-optimal approach significantly reduced the number of experiments required by classic full- or fractional-factorial designs. These experiments are uniformly distributed over the three-dimensional variable space. The additional eight tests (17-24) in Table 1 were added to the design and represent opposing temperature conditions for those experiments not having a temperature pair in the first 16 runs. These 24 runs include all of the eight possible combinations of the three variables at extreme settings for both oxides, as well as the eight runs with at least one mid-level variable setting needed for non-linear modeling. Run 25 was added so that a dissolution rate for $UO_3 \cdot H_2O$ would be available at the same condition as already obtained for the other two oxides.

Both U_3O_8 and $UO_3 \cdot H_2O$ samples were powders because of the synthetic routes available for each. The U_3O_8 powders were National Bureau of Standards (NBS or NIST) Standard Reference Material (SRM) 750(b). U_3O_8 is the most stable of the uranium oxides and is easily produced by the well known method of heating a uranium compound, UO_2 in this case, to several hundred degrees Celsius in air. The dehydrated schoepite was synthesized via hydrolysis of analytical grade uranyl acetate in a glass distillation apparatus, with continuous additions of water to replace the acetic acid boiled off during the synthesis [6]. Surface areas of both were measured via the traditional BET method using xenon gas. The resulting surface area for the U_3O_8 is 0.18 ± 0.02 m^2/g and 0.31 ± 0.04 m^2/g for the $UO_3 \cdot H_2O$. X-ray Diffraction (XRD) of both materials indicated they were the correct phases. Particle size distributions were also determined by means of

sedimentation techniques. The median particle size for the U_3O_8 powder was 2.1 μm with a 25-75 percentile range of 1.0 to 2.8 μm. The median particle size for the $UO_3 \cdot H_2O$ powder was 4.1 μm with a 25-75 percentile range of 2.5 to 5.5 μm. The pore size of the filters used in the sample cells was 0.1 μm. This small pore size, combined with the upward flow of the aqueous solution at a slow velocity of ~3-15 cm/hr, kept the particles within the sample cells.

Test solutions were prepared using analytical-reagent grade chemicals and deionized water. Each solution was continuously sparged with argon gas containing fixed concentrations of oxygen and carbon dioxide to maintain the desired dissolved oxygen concentration and pH of the solution. The test solutions flowed through stainless steel sample cells at rates between 5 and 25 mL/hr. Several times per week, effluent from the cells was collected, acidified to prevent uranium adsorption on the sample vial walls, and analyzed for uranium content using a phosphorescence analyzer. Dissolution rates were calculated from uranium concentrations multiplied by flow rates and divided by surface areas of the test specimens. After steady-state dissolution rates were achieved, the flow rates were occasionally changed to ensure that the observed dissolution rates remained unchanged. Dissolution rates will not be affected by changing flow rates, if the reaction is not solubility- or diffusion-limited.

RESULTS

The 25 measured dissolution rates of U_3O_8 and $UO_3 \cdot H_2O$ at atmospheric oxygen are shown in Table 1, as well as the actual values for the three independent variables, temperature, carbonate concentration and pH. Most experiments lasted about a month. The dissolution rates are the average values after reaching steady-state. The values preceded by an approximation or greater-than sign are estimates, because steady-state could not be reached or the sample was dissolving too rapidly. Rapid sample dissolution was particularly true for the dehydrated schoepite. Table 2 lists the uranium dissolution rates for the three oxides, UO_2 [2], U_3O_8 and $UO_3 \cdot H_2O$ that were measured under atmospheric oxygen conditions. Because the measured values of the independent variables differ between runs, only their nominal values are listed in Table 2. Two new room-temperature UO_2 results were measured at a pH of 10 and 2×10^{-4} and 2×10^{-2} molar total carbonate. These were acquired so that there would be a full set of eight measurements at the extreme conditions (a full-factorial linear experimental design) for each oxide. Results for a spent fuel [2], ATM-103, are listed at equivalent conditions. To facilitate easier comparisons of the dissolution rates and variable effects, the results for the eight experimental conditions at the high and low values of each variable are grouped together as Part 1 of Table 2. They are grouped first by pH, then by carbonate concentration and finally by temperature. Also included are three dissolution rates of UO_2, U_3O_7 and U_3O_8 at a commonly used condition of room-temperature, pH of 8, and 2×10^{-2} molar total carbonate that were estimated from figures in reference [7]. To avoid confusion in comparing trends, the remaining results at intermediate pH and carbonate concentrations are listed separately as Part 2 of Table 2 using the same grouping scheme.

The oxide phase has by far the strongest effect on the uranium dissolution rate. Because U_3O_8 has both U(IV) and U(VI) valence states, its dissolution rates might be expected to be between that of UO_2 and $UO_3 \cdot H_2O$, particularly as carbonate concentrations increase. Indeed, the rate increases significantly in going from UO_2 to U_3O_8 and dramatically from U_3O_8 to $UO_3 \cdot H_2O$. The $UO_3 \cdot H_2O$ dissolution is so rapid that the samples disappear within a few days at the high carbonate levels. With the U_3O_8, unlike UO_2, carbonate affects the dissolution rate to a greater extent than does temperature. Increasing temperature shows its expected effect of enhancing the dissolution rate. The enhancement is particularly strong at the highest carbonate concentration. The data indicate that alkaline pH is the least significant factor in dissolution of spent fuel or any of the uranium oxides under the alkaline conditions of these experiments, although it seems more important in $UO_3 \cdot H_2O$ dissolution. The $UO_3 \cdot H_2O$ dissolution data show strong nonlinearities in dissolution response to all of the variables, pH, temperature and carbonate concentrations. These nonlinearities may only be due to the difficulties in determining appropriate $UO_3 \cdot H_2O$ dissolution rates. A comparison of the leachate and prepared solution pH's of the $UO_3 \cdot H_2O$ experiments in

Table 2 shows that the solution pH sometimes drops upon contact with $UO_3 \cdot H_2O$, particularly at low carbonate concentrations. Nuclear Magnetic Resonance (NMR) analysis of the $UO_3 \cdot H_2O$ shows no residual acetate that might cause the acidity. The $UO_3 \cdot H_2O$ may act as a Brønsted acid by donating a proton, but the actual cause of the acidity is not known. Where the carbonate concentration is low, there is less buffering capacity of the solution.

MODELING

Only the fourteen U_3O_8 dissolution rate data given in Table 2 were modeled. Because the $UO_3 \cdot H_2O$ dissolved so rapidly, their dissolution rates are estimates or minima and not appropriate for modeling. As with the UO_2 dissolution data several approaches to U_3O_8 dissolution modeling are being explored. Again the classical observed chemical kinetic rate law was used and takes the following well-known general form [8]:

$$\text{Rate} = k[A]^a[B]^b[C]^c...\exp(-E_a/RT), \quad (1)$$

This generalized form of the rate law is for homogeneous gas or liquid reaction systems. It does not take into consideration the possibly complex liquid-solid reaction at the UO_x or spent fuel surface. Additional term(s) are needed to account for this element of the reaction, and any radiation effects in the spent fuel, but they are unknown at this time.

Other function forms are being considered. Dissolution of a solid is a thermodynamic nonequilibrium process. An Onsager-type thermodynamic function provides a classical relationship for dissolution rate and is linearly related to the energy change of the solid dissolving into a liquid. This is expected to be descriptive of dissolution response close to thermodynamic equilibrium, particularly those controlled by diffusion kinetics. A form of the Butler-Volmer equation, used in correlation of corrosion and electrochemical rate data, is also being examined. The normal derivation of the Butler-Volmer equations assumes that the electrochemical processes are not at, but near, thermodynamic equilibrium. The Butler-Volmer equations are expected to be descriptive of energy-dependent surface reactions.

Only regression fits of the U_3O_8 dissolution rate data to the classical chemical kinetic rate law are discussed here, for comparison with the previously reported UO_2 and spent fuel models. Model parameters are presented, based on both the leachate pH's used in the UO_2 dissolution models, and the pH's of the original carbonate solutions, before contact with the UO_2 or spent fuel samples, as used previously for the spent fuel data. The pH's of the fresh carbonate leaching solutions are probably more representative of the pH at the sample than the pH of the leachate analysis sample that has been exposed to dissolved CO_2 from the air.

The following equation was fitted using the measured leachate pH's given in Table 1:

U_3O_8 (leachate pH's):

$$\log_{10}(DR)\{mgU/m^2 \cdot day\} = 7.832 + 0.6910 \cdot \log_{10}[CO_3] + 0.0860 \cdot \log_{10}[H] - 1317/T$$

$r^2=0.87.$ (2)

Using the pH's of the prepared carbonate solutions, also given in the same column of the table, we arrive at similar, but perhaps more accurate, coefficients:

U_3O_8 (carbonate soln. pH's):

$$\log_{10}(DR)\{mgU/m^2 \cdot day\} = 7.951 + 0.6492 \cdot \log_{10}[CO_3] + 0.1065 \cdot \log_{10}[H] - 1333/T$$

$r^2=0.88.$ (3)

As with the earlier UO_2 and spent fuel dissolution data, the pH did not have much effect on the model. However, carbonate concentration, not temperature, had the strongest effect on the U_3O_8 dissolution rate. The temperature had half the effect of carbonate concentration on the uranium dissolution rate. The pH was only about one-sixth as effective as carbonate concentration in explaining the changes in U_3O_8 dissolution rates. Leaving out the pH term had a negligible effect on the other coefficients and was absorbed in the constant:

U_3O_8 (carbonate soln. pH's):

$$\log_{10}(DR)\{mgU/m^2 \cdot day\} = 6.925 + 0.6486 \cdot \log_{10}[CO3] - 1307/T$$

$r^2=0.86.$ (4)

Temperature and carbonate concentration show significant interaction. The pH shows its importance through interaction with carbonate as well. Additions of cross terms for those interactions to equation 4 improves the fit significantly, with a correlation coefficient of 0.95.

To allow comparisons with this U_3O_8 dissolution data, the previously reported spent fuel and UO_2 atmospheric oxygen models [2] are reproduced in equations 5 and 6. For consistency the UO_2 20% oxygen data were refitted using the fresh carbonate solution pH's and is shown in eq.7. This regression fit had a increased correlation coefficient, compared with the original fit using the leachate pH's (eq. 6). There was a larger change in the coefficients, than with the U_3O_8 results fitted with the two pH sets.

Spent Fuel, ATM-103 (20% oxygen only, carbonate soln. pH's):

$$\log_{10}(DR)\{mgU/m^2 \cdot day\} = 7.202 + 0.2260 \cdot \log_{10}[CO3] + 0.0905 \cdot \log_{10}[H] - 1628/T$$

$r^2=0.95.$ (5)

UO_2 (20% oxygen only, leachate pH's):

$$\log_{10}(DR)\{mgU/m^2 \cdot day\} = 4.650 + 0.2742 \cdot \log_{10}[CO3] - 0.1868 \cdot \log_{10}[H] - 1501/T$$

$r^2=0.79.$ (6)

UO_2 (20% oxygen only, carbonate soln. pH's):

$$\log_{10}(DR)\{mgU/m^2 \cdot day\} = 5.828 + 0.3335 \cdot \log_{10}[CO3] - 0.1571 \cdot \log_{10}[H] - 1734/T$$

$r^2=0.83.$ (7)

CONCLUSIONS

The aim of this work has been the measurement of the intrinsic dissolution rates of uranium oxides under a variety of well-controlled conditions. These experiments are relevant to a geological repository and allow for modeling. After exposure to air at elevated temperature, the stable phase U_3O_8 may form from spent fuel. Formation of dehydrated schoepite, $UO_3 \cdot H_2O$, has been found in drip tests with spent fuel.

Equivalent sets of U_3O_8 and $UO_3 \cdot H_2O$ dissolution experiments allowed a systematic examination of the effects of temperature (25-75°C), pH (8-10) and carbonate ($2\text{-}200 \times 10^{-4}$ molar) concentrations at atmospheric oxygen conditions.

Results indicate that $UO_3 \cdot H_2O$ has a much higher dissolution rate (at least ten-fold) than U_3O_8. Dissolution of both U_3O_8 and $UO_3 \cdot H_2O$ shows a very high sensitivity to carbonate concentration. Present results show a 25 to 50-fold increase in room-temperature $UO_3 \cdot H_2O$ dissolution rates between the highest and lowest carbonate concentrations. The intrinsic dissolution rate of

unirradiated U_3O_8 is about twice that of UO_2 under similar conditions. At the frequently-studied condition of room temperature, pH of 8, and 2 x 10^{-2} molar total carbonate, this data and the room-temperature dissolution rates of UO_2, U_3O_7, and U_3O_8 estimated from figures in reference [7] show a consistent increase in the intrinsic dissolution rates as the degree of oxidation increases.

As with the UO_2 dissolution data the classical observed chemical kinetic rate law was used to model the U_3O_8 dissolution rate data. The pH did not have much effect on the models, in concert with the earlier UO_2 and spent fuel dissolution data,. However, carbonate concentration, not temperature, had the strongest effect on the U_3O_8 dissolution rate. The U_3O_8 dissolution activation energy was about 6000 cal/mol, compared with 7300 and 8000 cal/mol for spent fuel and UO_2 respectively.

ACKNOWLEDGMENTS

Work performed under the auspices of the U.S. Department of Energy by Lawrence Livermore National Laboratory under Contract W-7405-ENG-48. This work was supported under activities D-20-53 of the Yucca Mountain Project Spent Fuel Waste form Task (YMP WBS element 1.2.2.4.1) and the AECL/USDOE Cooperative Project sponsored by the DOE Office of Civilian Radioactive Waste Management.

REFERENCES

1. P.A. Finn et al., Proc. of Topical Meeting on DOE Spent Nuclear Fuel, Salt Lake City, UT, pp. 421-429 (1994).

2. S. A. Steward and W. J. Gray, Proc. 5th Annual Intl. High-Level Radio. Waste Mgmt. Conf., **4**, 2602-8 (1994).

3. W.J. Gray, H.L. Leider and S.A. Steward, J. Nucl. Mater., **190**, 46-52 (1992).

4. S. A. Steward and H. C. Weed, in Scientific Basis for Nuclear Waste Management XVII, edited by A. Barkatt and R. A. Van Konynenburg (Mater. Res. Soc. Proc. **333**, Pittsburgh, PA, 1994) pp. 409-416.

5. BBN Software Products Corporation, RS/Discover, Version 2 (1989).

6. K. H. Gayer and H. Leider, JACS, **77**, 1448 (1955).

7. W. J. Gray, L. E. Thomas and R. E. Einziger, in Scientific Basis for Nuclear Waste Management XVI, edited by C. G. Interrante and R. T. Pabalan, (Mater. Res. Soc. Proc. **294**, Pittsburgh, PA, 1993) pp. 47-54.

8. W. Stumm and J. J. Morgan, Aquatic Chemistry: An Introduction Emphasizing Chemical Equilibria In Natural Waters, 2nd ed. (John Wiley and Sons, New York , 1981), Chapter 2.14.

Table 1. Test Matrix for the UO_{2+x} Dissolution Tests.

RUN	OXIDE	TEMPERATURE (deg C)	CARBONATE (mol/L)	PH Meas./Soln.	DISSOLUTION RATE ($mgU/m^2 \cdot day$)
1	U_3O_8	22.9	0.02	8.6/8.0	19
2	$UO_3 \cdot H_2O$	24.9	0.02	10.0/10.0	~200
3	U_3O_8	74.8	0.02	10.3/10.0	~200
4	$UO_3 \cdot H_2O$	74.7	0.02	8.6/8.0	>1500
5	U_3O_8	22.9	0.0002	8.9/10.0	0.8
6	$UO_3 \cdot H_2O$	24.9	0.0002	7.3/8.0	~100
7	$UO_3 \cdot H_2O$	74.7	0.0002	8.3/10.0	>150
8	U_3O_8	74.8	0.0002	8.1/8.0	~6
9	U_3O_8	22.9	0.02	10.6/10.0	21
10	$UO_3 \cdot H_2O$	24.9	0.0002	7.5/10.0	>100
11	$UO_3 \cdot H_2O$	74.7	0.02	10.0/10.0	>1000
12	U_3O_8	48.0	0.002	8.0/8.0	~10
13	U_3O_8	48.0	0.02	9.0/9.0	>100
14	$UO_3 \cdot H_2O$	25.0	0.002	9.0/9.0	~120
15	$UO_3 \cdot H_2O$	24.9	0.02	8.6/8.0	~700
16	U_3O_8	22.9	0.0002	8.4/9.0	1.3
17	$UO_3 \cdot H_2O$	74.7	0.0002	8.1/8.0	>200
18	U_3O_8	74.8	0.02	8.6/8.0	~150
19	U_3O_8	74.8	0.0002	9.3/10.0	~3
20	U_3O_8	74.8	0.0002	8.1/10.0	~4
21	U_3O_8	21.6	0.002	8.6/8.0	~10
22	U_3O_8	21.6	0.02	9.2/8.0	8.3
23	$UO_3 \cdot H_2O$	75.0	0.002	9.0/ 9.0	>20
24	U_3O_8	22.9	0.002	7.9/8.0	~5
25	$UO_3 \cdot H_2O$	25.0	0.02	9.0/9.0	>1500

Table 2, Part 1. Comparison of Dissolution Rates at Boundary Conditions

pH	Carbonate (mol/L)	Oxygen (atm)	Temp °C	Dissolution Rates ($mgU/m^2 \cdot day$) Spent Fuel ATM-103 [2]	UO_2	U_3O_8	$UO_3 \cdot H_2O$
8	0.0002	0.2	25		3.9	~5	~100
8	0.0002	0.2	50		5.4		
8	0.0002	0.2	75	8.6	11	~6	>200
8	0.02	0.2	25	3.5	2.4 (~3)[a]	[U_3O_7 (~3-5)[a]] 19 (~10-15)[a]	~700
8	0.02	0.2	50		38		
8	0.02	0.2	75		54	~150	>1500
10	0.0002	0.2	25	0.63	2.5	0.8	>100
10	0.0002	0.2	50		3.1		
10	0.0002	0.2	75		6.5	~3	>150
10	0.02	0.2	25		20	21	~200
10	0.02	0.2	50		26		
10	0.02	0.2	75	14	77	~200	>1000

a) See reference 7 for estimated rates in parentheses, including U_3O_7.

Table 2, Part 2. Comparison of Dissolution Rates at Intermediate Conditions

pH	Carbonate (mol/L)	Oxygen (atm)	Temp °C	Dissolution Rates ($mgU/m^2/day$) Spent Fuel ATM-103 [2]	UO_2	U_3O_8	$UO_3 \cdot H_2O$
8	0.002	0.2	25			~10	
8	0.002	0.2	50			~10	
9	0.0002	0.2	25			1.3	
9	0.0002	0.2	75			~4	
9	0.002	0.2	25				~120
9	0.002	0.2	50	6.1	12		
9	0.002	0.2	75		23		>20
9	0.02	0.2	25	2.8	6.7	8.3	>1500
9	0.02	0.2	50			>100	
10	0.002	0.2	25	2.0	9.3		

Technical Information Department · Lawrence Livermore National Laboratory
University of California · Livermore, California 94551

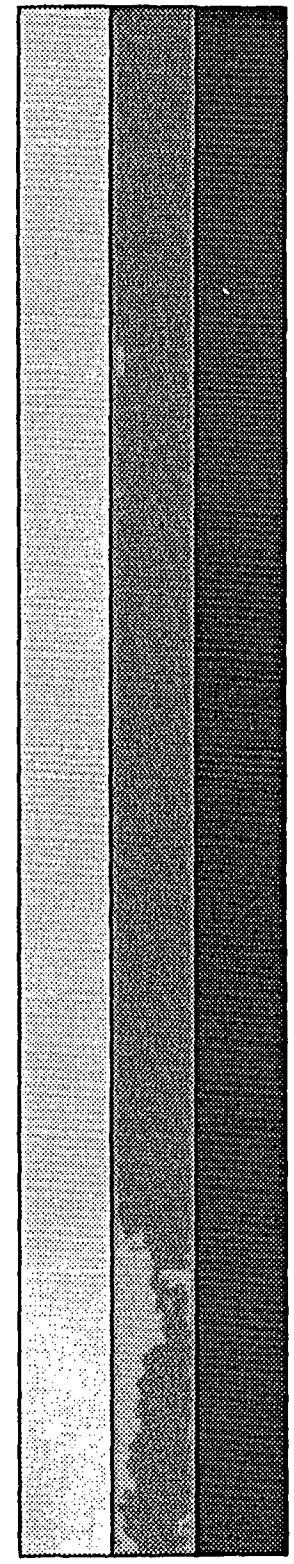

Recycled
Recyclable